Photoluminescence spectroscopy and decay time measurements of polycrystalline thin film CdTe/CdS solar cells

C. J. Bridge, P. Dawson, P. D. Buckle, and M. E. Özsan

Photoluminescence spectroscopy and decay time measurements of polycrystalline thin film CdTe/CdS solar cells

C. J. Bridge, P. Dawson,[a] and P. D. Buckle
Department of Physics, UMIST, P.O. Box 88, Manchester M60 1QD, England

M. E. Özsan
BP Solar, 12 Brooklands Close, Windmill Road, Sunbury-on-Thames TW16 7DX, England

The results of room temperature photoluminescence spectroscopy and decay time measurements carried out on CdTe/CdS solar cells are reported. The as-grown structures were annealed in air at temperatures in the range 350–550 °C. For excitation via the CdTe/CdS interface, longer photoluminescence decay times were observed as the anneal temperature was increased, this is attributed to localized passivation of nonradiative states possibly due to the effect of S interdiffusion. When the photoluminescence is excited via the CdTe free surface, the decay curves consist of a fast and slow component. The fast component (<130 ps) of the photoluminescence is attributed to nonradiative recombination at grain boundaries or the CdTe free surface. The slow component is attributed to the effects of carrier drift and diffusion and subsequent recombination at the CdTe/CdS interface. Modeling of the transport process has led to the extraction of a value of 0.20 ± 0.03 cm^2 s^{-1} for the minority carrier diffusion coefficient of the CdTe for the sample annealed at 450 °C. These results are correlated with improvements in device efficiency determined from illuminated current density–voltage measurements. © *2000 American Institute of Physics.*
[S0021-8979(00)07024-9]

I. INTRODUCTION

Thin film solar cells are of commercial interest because of their potential as a means of large scale, low cost, power generation. CdTe is a promising thin film device material because of its near ideal room temperature band gap (1.5 eV) and its high absorption coefficient. At present large area CdTe solar cells are generally based on CdTe/CdS heterostructures, in most cases heat treatment, either postgrowth or during the film deposition stage, is required to achieve high conversion efficiencies. The effects of such treatments, however, are only qualitatively understood and vary for different deposition techniques.[1]

Efficiencies in excess of 16% have been reported[2] for small area (0.02 cm^2) CdTe/CdS solar cells and large area modules (30 cm×30 cm) can have efficiencies of 10%. Central to the achievement of high efficiencies is the postgrowth anneal in air at temperatures of up to 500 °C of as grown material. Principally, the annealing leads to the formation of a $p-n$ heterojunction through type conversion of the n type CdTe.[3,4] However, S and Te intermixing in the junction region, recrystallization, and grain growth have also been reported[5,6] and may be beneficial to device performance via the reduction of nonradiative recombination.

A particularly useful way to study nonradiative recombination processes is to monitor the photoluminescence decay following excitation by a pulse of light. This technique was used by Ahrenkiel and co-workers[7] who showed that nonradiative recombination at grain boundaries is an important recombination mechanism in polycrystalline CdTe/CdS solar cells.

In this study we report photoluminescence decay measurements that have been carried out on a range of CdTe/CdS solar cell structures to investigate how the annealing temperature influences the carrier recombination dynamics. In order to probe different regions of the structures the experiments were performed using either excitation of the CdTe free surface or excitation via the CdTe/CdS interface. The results of the optical measurements have been correlated with device efficiency determined from illuminated current density–voltage measurements.

II. EXPERIMENTAL DETAILS

A schematic diagram of a device structure is shown in Fig. 1. The structures were fabricated as follows. First a thin ($\sim$1000 Å) ''window'' layer of n type CdS was deposited by chemical bath deposition on a tin–oxide coated glass substrate. This was then followed by the electrodeposition of an n type CdTe film (1.6 ± 0.1 μm). The as deposited samples were annealed in air at temperatures up to 550 °C for 15 min and then contacted using carbon paste. Current density–voltage characteristics were carried out under 100 mW/cm^2 illumination using a quartz–halogen lamp to determine the device efficiency.

The photoluminescence decay data were obtained by exciting the CdTe layer (at the free surface or via the CdTe/CdS interface) with a cavity dumped, mode-locked dye laser (photon energy=2.14 eV, i.e., less than the band gap of the CdS) at a pulse repetition rate of 300 kHz and with a pulse width of $\leq$10 ps. The 1/e absorption depth of the exciting

[a]Author to whom correspondence should be addressed; electronic mail: philip.dawson@umist.ac.uk
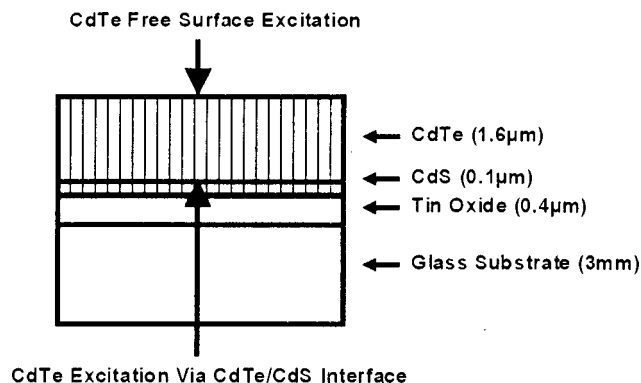
FIG. 1. Schematic cross section of the CdTe/CdS solar cell structures. The arrows indicate the direction of the incident laser beam used for the different excitation geometries.
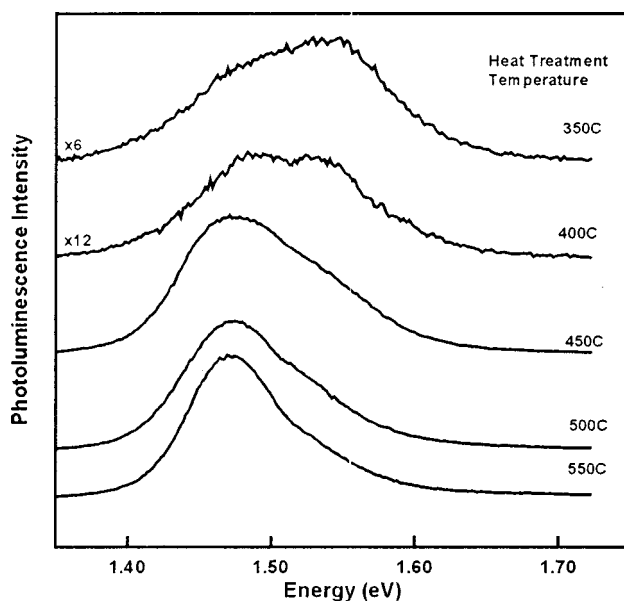

FIG. 2. Room temperature time integrated photoluminescence spectra as a function of sample anneal temperature obtained using via excitation of the CdTe/CdS interface.

radiation in the CdTe was estimated to be 0.1–0.2 μm; this is much less than the CdTe film thickness and so the majority of the photoexcited electron/hole pairs are created close to the CdTe free surface or the CdTe/CdS interface. Time correlated single photon counting was used to process the signal which was detected using a cooled S1 microchannel plate photomultiplier via a 0.75 m single grating spectrometer. The minimum measurable decay time using this arrangement was ~130 ps. Excitation densities were in the region of 10^{12}–10^{13} photons/cm^2/pulse.

The time integrated photoluminescence spectra were taken under identical conditions with the excitation chopped by a mechanical wheel and lock-in detection used to measure the photoluminescence intensity. The optical experiments were carried out on samples annealed in the temperature range 350–550 °C for steps of 25 °C. For the sake of clarity not all the data are presented in the following.

III. RESULTS AND DISCUSSION

A. Device performance

For anneal temperatures below 350 °C the device efficiency was found to be essentially zero. For anneal temperatures greater than 350 °C the results of the efficiency measurements are shown in Table I. The measured efficiencies are significantly lower than the highest reported values for structures of this type. This is largely due to low fill factors, believed to result from high resistance back contacts. Nonetheless, the anneal temperature of 500 °C, for which the best device is obtained, is consistent with the optimum anneal temperature reported previously for this type of structure.[3,6] In fact it should be stressed that solar cells fabricated from the same material used here grown at 500 °C and contacted

TABLE I. The dependence of device efficiency on anneal temperature.

Anneal temperature (C)	Device efficiency (%)
350	<0.1
400	0.2
450	4.0
500	5.2
550	3.0

using a commercial contacting procedure showed an efficiency of 11%. So we believe that the systematic changes in device performance are caused by changes in the material properties as a function of the heat treatment temperature. The marked improvement in efficiency between 400 and 450 °C is largely attributed to the *n*- to *p*-type conversion process in the CdTe leading to the formation of a $p-n$ junction.[3,4] Additional improvements may be due to enhanced quality of the heterointerface, e.g., from the effects of recrystallization/grain growth or sulphur interdiffusion as described later. The subsequent falloff in performance above 500 °C is caused by lift-off of the heterostructure from the tin–oxide rather than to any material degradation.

B. Room temperature photoluminescence spectroscopy and decay measurements

1. Excitation via the CdTe/CdS interface

The photoluminescence intensity was very weak or negligible for samples annealed below 350 °C. The time integrated photoluminescence spectra for anneal temperatures in the range 350–550 °C are shown in Fig. 2. The peak energy of the spectrum for the sample annealed at 350 °C of 1.55 eV is identical to the peak energy of the spectrum for the same sample when excited at the free surface (as discussed later). We attribute this recombination to being from the CdTe layer. The peak energy of 1.55 eV is greater than the band gap of CdTe and we attribute the shift to higher energy of the PL peak as being due to the effects of strain. However, an additional low energy shoulder is observed at around 1.5 eV. As the anneal temperature was increased this low energy shoulder was found to increase in intensity, such that for anneal temperatures in excess of 400 °C it became the dominant transition. This low energy feature also shifts to lower energy with increasing anneal temperature. We attribute the peak at low energy to recombination at the CdTe/CdS inter-
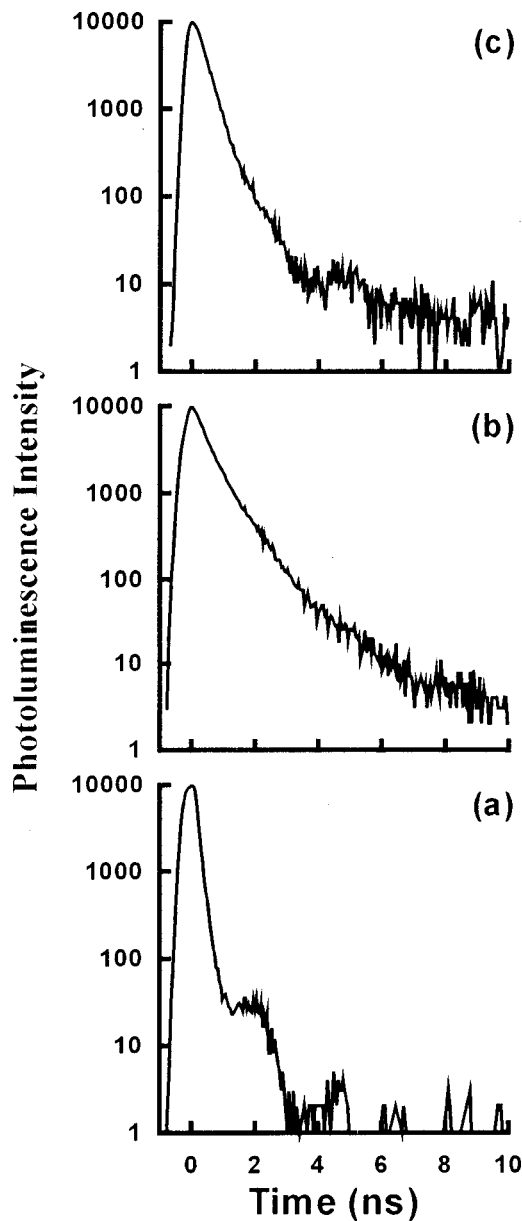
FIG. 3. Room temperature photoluminescence decay curves for excitation via the CdTe/CdS free surface for anneal temperatures of: (a) 400 °C, (b) 450 °C, and 500 °C.
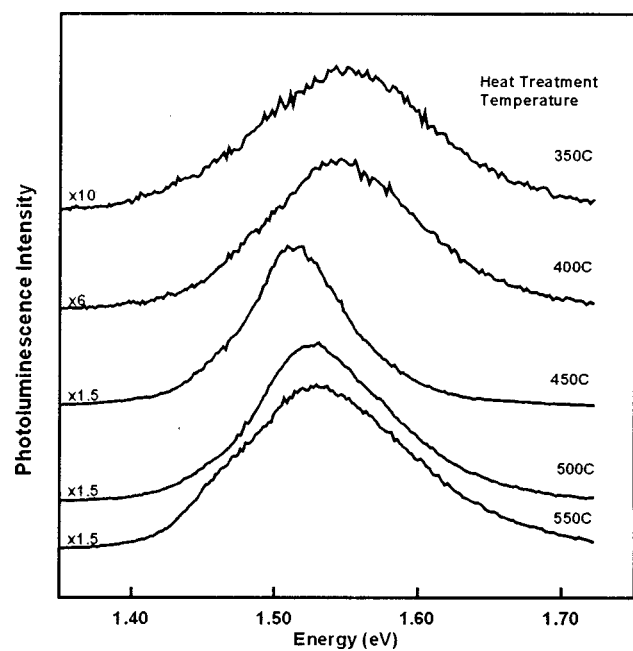

FIG. 4. Room temperature time integrated photoluminescence spectra as a function of sample anneal temperature obtained from excitation via the CdTe free surface.

initial decay for the samples annealed at 400 °C is an experimental artifact. As the anneal temperature is increased to 450 °C the decay curves become longer. The longer decay times (and corresponding increase in photoluminescence intensity) are attributed to a reduction in nonradiative recombination in the CdTe/CdS region. The reason for this improvement has not been conclusively established although the involvement of S interdiffusion would be an obvious possibility. Indeed, a reduction in the density of nonradiative CdTe/CdS interface states due to strain relaxation has been previously suggested as a likely consequence of S interdiffusion.[10] The subsequent shortening of the decay curves at anneal temperatures of 500 °C is ascribed to increased carrier sweepout. This would be expected due an increase in the internal electric field at these anneal temperatures through enhancement of the degree of type conversion in the CdTe layer.[3,4]

2. CdTe free surface excitation

For anneal temperatures below 350 °C no photoluminescence could be detected at room temperature. The time integrated spectra for this excitation configuration are shown in Fig. 4; for anneal temperatures >350 °C photoluminescence spectra with a peak energy ~1.53 eV could be observed. The progressive increase in photoluminescence intensity with anneal temperature indicates significant reductions in nonradiative recombination. The reason for the shift in peak position (1.54–1.52 eV) with anneal temperature is unclear. One possible explanation could involve recrystallization of the CdTe, which could lead to changes in strain within the CdTe grains.

The decay of the photoluminescence observed from the samples annealed at temperatures of 400, 450, and 500 °C are shown in Fig. 5. The decay curves were measured on the low energy side (detection energy 1.44 eV) of the peak of the

face. The shift to lower energy is attributed to the effects of S interdiffusion into the CdTe from the CdS, which forms a $CdTe_{1-x}S_x$ alloy at the CdTe/CdS interface.[5] For $x<0.3$ this leads to a reduction in the energy band gap of the CdTe.[8] A shift of 10 meV relative to the original photoluminescence peak position corresponds to an increase in x of 0.01 for small values of x. Our results therefore indicate a S content in the interface region of around 3% for an anneal temperature of 350 °C increasing to 5% for the highest anneal temperature. Similar results have been reported previously for S interdiffusion in CdTe/CdS heterostructures.[9]

Figure 3 shows the photoluminescence decay curves for excitation via the CdTe/CdS interface at a detection energy of 1.44 eV for samples annealed at 400, 450, and 500 °C. For anneal temperatures <400 °C all the decay curves were identical to that shown in Fig. 3(a); note the feature after the
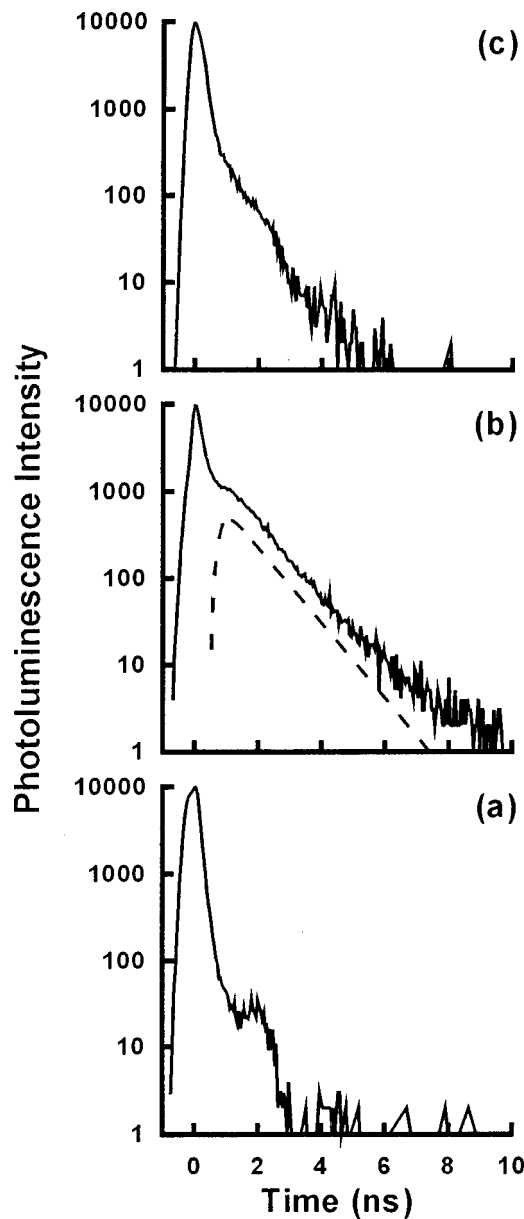
FIG. 5. Room temperature photoluminescence decay curves for excitation via the CdTe free surface for anneal temperatures of: (a) 400 °C, (b) 450 °C, and (c) 500 °C. The result (−−) from the carrier transport model is shown for the sample annealed at 450 °C.

spectra; the reason for this is explained in Sec. III. Depending on the anneal temperature the decays curves consist of either a single fast component or a combination of fast and slow components. Determination of the time constant of the fast component was limited by the system response, i.e., 130 ps. For anneal temperatures of 450 °C and above, a longer, secondary decay component was also observed; this will be discussed in detail in Sec. III. For the purposes of the discussion in this section we ascribe the fast decay component to carriers that recombine in the CdTe layer.

In general the photoluminescence decay time can be described in terms of the sum of radiative and nonradiative recombination lifetimes such that

$$\frac{1}{\tau_{PL}} = \frac{1}{\tau_R} + \frac{1}{\tau_{NR}},$$

where τ_{PL} is the measured decay time and τ_R and τ_{NR} are the radiative and nonradiative lifetimes, respectively.

Assuming free carrier recombination, under low injection conditions

$$\tau_R = \frac{1}{Bp},$$

where B is the radiative decay coefficient and p is the free hole concentration. Estimates[11,12] for B in CdTe lie in the region of 10^{-9} cm^{-3} s^{-1}. Using a figure of 10^{15} cm^{-3} for the free hole concentration[3] suggests a radiative lifetime in this material on the order of 1 μs for suitably low injection conditions. The fact that the fast component decay time is many orders of magnitude shorter than this suggests that recombination is predominantly nonradiative. The identification of the particular nonradiative process(es) involved is difficult and can be only the subject of speculation. While bulk non-radiative recombination cannot be ignored, the polycrystalline nature of the CdTe together with the exposed free surface suggest that grain boundary or surface recombination are likely to be the dominant decay processes. Indeed, non-radiative recombination at grain boundaries was held to be the dominant process in previous photoluminescence decay measurements on polycrystalline CdTe/CdS solar cells carried out by Ahrenkiel and co-workers.[7] In the work of Ahrenkiel *et al.* the measured lifetimes showed a geometric dependence on grain size with the excitation of larger grains (2 μm) at the interface, leading to longer lifetimes (>1 ns) compared to the excitation of smaller grains at the free surface (<1 ns). These results were explained using a spherical grain model where the photoluminescence lifetime was dependent on grain diameter, minority carrier diffusion coefficient, and surface recombination velocity (SRV).

This type of analysis has been applied to our CdTe films. The grains in our structures are columnar in structure and much narrower (~0.15 μm across)[13] than the spherical grains described by Ahrenkiel *et al.* To a first approximation such grains can be described as cuboids with dimensions a, b, and c. Van Opdorp's analysis[14] of nonradiative recombination between two plan parallel surfaces of infinite SRV and separated by a distance a leads to a surface recombination lifetime given by

$$\frac{1}{\tau_a} = \frac{\pi^2 D}{a^2},$$

where D is the minority carrier diffusion coefficient. By extending this expression to three dimensions (i.e., the three pairs of surfaces that comprise the cuboid), the surface/grain boundary lifetime τ can be shown[15] to be given by

$$\frac{1}{\tau} = \pi^2 D \left[\frac{1}{a^2} + \frac{1}{b^2} + \frac{1}{c^2} \right].$$

Substituting the value of D determined in Sec. III into this expression yields a surface/grain boundary recombination lifetime of ~50 ps. Therefore, grain boundary/surface recombination could easily account for the short photoluminescence decay lifetimes (<130 ps) observed in our measurements.
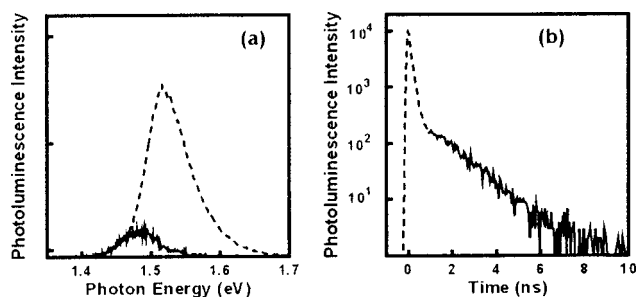
FIG. 6. (a) Time resolved photoluminescence spectra for the fast (−−) and the slow (—) time windows for the sample annealed at 450 °C; (b) the decay of the photoluminescence intensity detected at a energy of 1.44 eV with the fast decay component (−−−) and the slow decay component (——).

3. Secondary decay component from CdTe free surface excitation

The two decay components observed using CdTe free surface excitation is due to the photoluminescence spectrum consisting of two overlapping components. Of particular relevance is the fact that the secondary slow decay observed using free surface excitation for anneal temperatures >450 °C is similar to the photoluminescence decay curve observed using interface excitation at the same anneal temperatures. Figure 4 shows the time integrated photoluminescence spectrum obtained using CdTe free surface excitation for the sample annealed at 450 °C. The peak of the spectrum is at 1.52 eV. The form of the photoluminescence decay associated with the free surface excitation was found to exhibit a distinct spectral dependence. Measurements made on the high energy tail of the photoluminescence spectrum showed a single fast decay of ~130 ps. However, using lower detection energies (<1.5 eV) saw the emergence of an additional, slower component which became progressively more dominant as the detection energy was reduced. Figure 6(b) shows the photoluminescence decay curve for a detection energy of 1.44 eV where the fast and slow components can be easily seen.

Using time resolved spectroscopy the spectra associated with the two decay components can be identified by defining ''fast'' (0–250 ps) and ''slow'' (3500–8000 ps) detection windows; the results of the time resolved spectroscopy are shown in Fig. 6(a). The fast decay component gives rise to a luminescence spectrum with the same peak position as the time integrated photoluminescence spectrum. The slower, secondary component however, is associated with a much weaker, overlapping feature with a peak energy of 1.48 eV. This is at the same energy as the peak of the spectrum measured using interface excitation that has been ascribed previously to recombination involving the CdS_xTe_{1-x} layer (see Fig 2). Not only is the time integrated spectrum using CdTe/CdS interface excitation and the slow time resolved spectrum using free surface excitation the same, but the form of the time decay curves are also the same, ignoring the fast component in the free surface excitation geometry. Thus we propose that the slowly decaying component with a peak energy at 1.48 eV observed using the free surface excitation geometry is due to recombination in the intermixed CdS_xTe_{1-x} layer. This we believe is due to the combined effects of drift

and diffusion of carriers excited at the CdTe free surface. These transport effects are responsible for causing the time delay following excitation that causes the ''hump'' in the data in Fig. 6(b). Measurements carried out on the samples annealed at higher temperatures also showed qualitatively the same behavior.

A Monte Carlo simulation was developed to model the secondary photoluminescence decay process observed from free surface excitation of the CdTe film. Although experimentally the initial injection density per pulse is around an order of magnitude greater than the CdTe free carrier density, the proportion of photoexcited carriers that contribute to the slow decay process is orders of magnitude less than those that contribute to the initial fast photoluminescence decay. Consequently, it is assumed that the problem can be treated in terms of minority carrier transport and recombination.

A one dimensional array was used to represent the CdTe film and a narrow CdTeS region. Photoexcitation at $t=0$ was represented by filling the array according to an exponentially decaying carrier concentration profile determined using an absorption coefficient of 5×10^4 cm^{-1}. By assigning a numerical range for movement left, right, or not at all within the array, carrier diffusion was modeled using a random number generator to define the motion of each carrier in the system for every time step. Probabilities were weighted in one direction to account for the effect of the electric field in the depletion region.

The extent of the depletion region and the electric field strength were estimated from Poisson's equation using a carrier concentration of 10^{15} cm^{-3}. Infinite SRV was assumed at the CdTe free surface while carriers reaching the interface side were fed into the narrow CdTeS layer. The recombination time for carriers in the CdTe film was included using a value of 130 ps (albeit an upper limit), i.e., the decay time measured using the free surface excitation geometry. The recombination rate in the CdTeS layer was included using the decay rate observed from interface excitation measurements. The diffusion coefficient D was incorporated as a variable parameter. By varying D the position of the ''hump'' characterizing the delay associated with the secondary decay could be fitted to the experimental data.

A comparison of the results of our model with the experimental data (shown in Fig. 5) was complicated by the presence of the fast initial photoluminescence decay which masked the rise of the secondary component. Nevertheless, the best fit to the 450 °C annealed sample yielded a value of D of 0.20 ± 0.03 cm^2/s. It was not possible to estimate D for anneal temperatures other than 450 °C with any degree of reasonable accuracy.

IV. SUMMARY AND CONCLUSIONS

Photoluminescence time decay measurements have been carried out on polycrystalline CdTe/CdS solar cells for a range of postgrowth anneal temperatures. For anneal temperatures of 400 °C and below, the decay of the CdTe band edge photoluminescence, using both CdTe free surface and

CdTe/CdS interface excitation, is dominated by a fast decay. This suggests that carrier recombination is predominantly nonradiative which we attribute to grain boundary/surface recombination.

At anneal temperatures of 450 °C and above, a longer photoluminescence decay is measured using interface excitation. The lengthening of the interface photoluminescence decay is believed to be a result of the passivation of nonradiative interface/grain boundary states in the CdTe/CdS interface region. This observation coincides with a considerable increase in device efficiency although this is, in part, believed to be due to type conversion of the CdTe.

The interface photoluminescence decay is also manifested as a delayed secondary component in photoluminescence decay curves measured using free surface excitation, suggesting carrier transport across the CdTe film to the CdTe/CdS interface. Modeling of this process has allowed a CdTe minority carrier diffusion coefficient of 0.2 ± 0.03 cm^2 s^{-1} to be extracted from the delay for the sample annealed at 450 °C.

ACKNOWLEDGMENT

[1] D. Bonnet, Int. J. Solar Energy **12**, 14 (1992).

[2] T. Aramoto *et al.*, Jpn. J. Appl. Phys., Part 1 **36**, 6304 (1997).

[3] B. M. Basol, J. Appl. Phys. **55**, 601 (1984).

[4] C. J. Bridge, P. Dawson, P. D. Buckle, and M. E. Ozsan, Semicond. Sci. Technol. **15**, 1 (2000).

[5] M. E. Özsan, D. R. Johnson, S. Oktik, M. H. Patterson, D. Sivapathasundaram, and J. M. Woodcock, Proceedings of the 12th European Photovoltaic Solar Energy Conference Amsterdam, 1994, p. 1604.

[6] M. E. Ozsan, D. R. Johnson, D. W. Lane, and K. D. Rogers, Proceedings of the 12th European Photovoltaic Solar Energy Conference, Amsterdam, 1994, p. 1600.

[7] R. K. Ahrenkiel, B. M. Keyes, L. Wang, and S. P. Albright, Proceedings of the 22nd IEEE Photovoltaic Specialists' Conference, Las Vegas, 1991, Vol. 22, p. 940.

[8] K. Ohata, J. Saraie, and T. Tanaka, Jpn. J. Appl. Phys. **12**, 1641 (1973).

[9] D. H. Levi, L. M. Woods, D. S. Albin, T. S. Gessert, D. W. Niles, A. Swartzlander, D. H. Rose, R. K. Ahrenkiel, and P. Sheldon, Proceedings of the 26th Photovoltaic Specialists Conference, New York, 351 (1997).

[10] Z. C. Feng, H. C. Chou, A. Rohatgi, G. K. Lim, A. T. S. Wee, and K. L. Tan, J. Appl. Phys. **79**, 2151 (1996).

[11] R. K. Ahrenkiel, B. M. Keyes, D. Levi, K. Emery, T. L. Chu, and S. S. Chu, Appl. Phys. Lett. **64**, 2879 (1994).

[12] R. Cohen, V. Lyahovitskaya, E. Poles, A. Liu, and Y. Rosenwaks, Appl. Phys. Lett. **73**, 1400 (1998).

[13] P. D. Buckle, C. J. Bridge, J. Jacobs, A. J. Harvey, U. Bangert, P. Dawson, E. Z. Luo, I. H. Wilson, and M. E. Ozsan, Inst. Phys. Conf. Ser. **106**, 641 (1999).

[14] C. van Opdorp, C. Werkhoven, and A. T. Vink, Appl. Phys. Lett. **30**, 40 (1977).

[15] H. S. Carslaw and J. C. Jaeger, *Conduction of Heat in Solids*, 2nd ed. (Clarendon, Oxford, 1959).